Linköping University Post Print

Industrial-scale deposition of highly adherent CN_x films on steel substrates

Esteban Broitman, Zs. Czigany, Grzegorz Greczynski, J. Bohlmark,
R. Cremer and Lars Hultman

N.B.: When citing this work, cite the original article.

Original Publication:

Esteban Broitman, Zs. Czigany, Grzegorz Greczynski, J. Bohlmark, R. Cremer and Lars Hultman, Industrial-scale deposition of highly adherent CN_x films on steel substrates, 2010, Surface & Coatings Technology, (204), 21-22, 3349-3357.
http://dx.doi.org/10.1016/j.surfcoat.2010.03.038
Copyright: Elsevier Science B.V., Amsterdam.
http://www.elsevier.com/

Postprint available at: Linköping University Electronic Press
http://urn.kb.se/resolve?urn=urn:nbn:se:liu:diva-58178

Industrial-scale deposition of highly adherent CN_x films on steel substrates

E. Broitman[1,2,†] , Zs. Czigány[3], G. Greczynski[1], J. Böhlmark[4], R. Cremer[5,] , L. Hultman[1]*

(1) IFM, Linköping University, SE-581 83 Linköping, Sweden.
(2) Department of Chemical Engineering, Carnegie Mellon University, Pittsburgh, PA 15213, USA.
(3) Research Institute for Technical Physics and Materials Science, H-1525 Budapest, Hungary.
(4) Sandvik Tooling R&D, SE-126 80 Stockholm, Sweden.
(5) CemeCon AG, D-52146 Würselen, Germany.

(†) Corresponding author.
(*) Present address: KCS Europe GmbH, D-52076 Aachen, Germany.

Abstract

Highly adherent carbon nitride (CN_x) films were deposited using a novel pretreatment with two high power impulse magnetron sputtering (HIPIMS) power supplies in a master-slave configuration: one to establish the discharge and one to produce a pulsed substrate bias. During the pretreatment, SKF3 (AISI 52100) steel substrates were pulse-biased in the environment of a HIPIMS Cr plasma in order to sputter clean the surface and to implant Cr metal ions. Subsequently, CN_x films were prepared at room temperature by DC unbalanced magnetron sputtering from a high purity graphite target in a N_2/Ar discharge at 3 mTorr. All processing was done in an industrial CemeCon CC800 system. A series of depositions were obtained with samples at different bias voltages (DC and pulsed) in the range 0-800 V. Scanning transmission microscopy (STEM) and high resolution transmission electron microscopy (HRTEM) show the formation of an interface comprising a polycrystalline Cr layer of 100 nm and an amorphous transition layer of 5 nm. The adhesion of CN_x films evaluated by the Daimler-Benz Rockwell-C reach strength quality HF1, and the scratch tests gives critical loads of 84 N. Adhesion results are correlated to the formation of an optimal interfacial mixing layer of Cr and steel.

KEYWORDS: carbon nitride, HIPIMS, HPPMS, adhesion, CN_x

PACS Codes: 68.35.Np, 81.15.-z, 81.05.U-, 81.15.Cd

1. INTRODUCTION

The scope of the present study is to overcome the problem of insufficient adhesion of carbon-based coatings on metal substrates. As a model system, we have selected carbon nitride (CN_x), which is proposed as the best candidate to replace diamond-like carbon (DLC) films due to their superior wear resistance, high hardness, and low friction coefficient [1]. The first successful industrial application of this material has been the use of very thin (~2-5 nm) films for the protection of hard disks [2, 3]. However, the scalability of CN_x coatings produced in laboratories to industrial engineering applications has been difficult as thicker films (1-5 μm) on steel substrates are required. The main reason is the development of high compressive intrinsic stresses during film growth which causes adhesion failures with delamination of films from the substrate surface [4].

The common practice to increase the adhesion of carbon-based coatings on steel substrates is to make a pretreatment of the substrates and the use of a metallurgical glue layer interposed between the surface substrate and the film. In this paper we study the deposition of highly adherent CN_x films on martensitic steel substrates using a novel high power impulse magnetron sputtering (HIPIMS) pretreatment where two HIPIMS power supplies are used in a master-slave configuration: one establish the discharge in the cathode and the second produces a pulsed substrate bias [5-7]. The plasma-processing methods used for improving adhesion of carbon-based coatings are reviewed from an historical point of view in Section 2. A description of our novel pretreatment and the experimental techniques are considered in Section 3. Section 4 presents the results and discussions, and 5 gives the conclusions.

2. PLASMA-PROCESSING PRETREATMENTS

In-situ surface preparation is an essential step in vacuum coating processing and is critical to assure a good adhesion film-substrate. For instance, air-exposed stainless steel is covered by a native oxide layer (from 1 to 5 nm thick) composed

of metal oxides and hydroxides [8]. Despite of pre-cleaning processes, other contaminants like organic and water molecules will also be present on the metal surface. Without the elimination of the oxide and contaminants, it is likely that any coating deposited on the surface will delaminate.

For many years, it has been known that cleaning of substrates using plasma techniques prior to physical vapor deposition processes can significantly improve coating adhesion. Such bombardment is expected not only to remove unwanted contaminant layers at the substrate surface, but also to create active dangling bonds, which may promote adhesion of the deposited film [9].

There are basically two different plasma processes that have been developed to *in-situ* clean substrates during PVD processing, namely: ion scrubbing and sputter cleaning [10, 11].

2.1. "Ion scrubbing"

The first *in-situ* plasma cleaning technique was developed in 1935 by Strong [12] for the cleaning of glass surfaces used in astronomical telescopes, and it is nowadays included in many commercial coating machines. The equipment consists of a DC high voltage "glow bar" that allows the formation of plasma. The surfaces in contact with the plasma acquire a negative voltage (several volts) with respect to the plasma. This sheath potential accelerates positive ions to the surface. When an ion contacts the surface it combines with electrons and releases its energy of ionization (5-20 eV). This low energy bombardment and heating desorbs adsorbed contaminants such as water vapor. The ion scrubbing can be done using argon or reactive gases like oxygen, chlorine, and hydrogen, the later are used to clean contaminants like hydrocarbons. In this technique, also known as "glow discharge cleaning" because of the light generated by the plasma, there is no bias voltage applied to the substrate [11].

2.2 "Sputter Cleaning"

In this technique ions generated in a plasma discharge are accelerated toward the surface held at a negative voltage; the ions clean the surface by

physical sputtering. In the beginning the technique was using gas ions accelerated by DC, RF, or pulsed-DC substrate biasing, but during the last decade, the development of new techniques like arc deposition and high power impulse magnetron sputtering (HIPIMS) allowed the simultaneous use of gas and metal ions [13].

2.2.1 Sputter cleaning by gas ions: DC biasing

One of the most successful techniques for adhesion enhancement has been the pre-treatment of the substrate surface with a low energy (500 eV) Ar^+ ions, *in situ* before vacuum vapor deposition of the films [14]. The first report of this technique is back to 1955, when Farnsworth *et al* [15] reported using sputter cleaning with Ar^+ ions to prepare ultra-clean surfaces for low-energy electron diffraction studies. Later, sputter cleaning was adopted by D. M. Mattox [16] to develop the "Ion-Plating" process. Mattox's process, with a filament used to evaporate a metal and a DC voltage used to accelerate the ions, evolved rapidly with the introduction of the DC magnetron sputtering technique for the deposition of thin films. Before deposition, the plasma cleaning is easily done by ions generated in the magnetrons, while the acceleration of the ions toward the substrate to be cleaned can be performed by a negative DC voltage applied to the substrate [17]. Figure 1a shows a typical process where the ions are generated by a magnetron cathode with a Cr target and the bias is provided by a negative DC voltage: the magnetron generates mainly Ar^+ ions because the efficiency of Cr ion generation is very low. In industrial production, where it is common to have a large deposition area, Ar^+ ions are usually provided by external sources. Anders [18] has recently reviewed some of these ion sources, such as hollow cathode discharges, linear sources of end-Hall type, and capacitively or inductively coupled plasma sources.

There are two drawbacks of this method. The first is the substrate heating during ion bombardment that can change, per example, the properties of some temperature sensitive substrates like steels. Another disadvantage is the incorporation of the gas ions into the substrate. An inert gas like Ar can occupy

interstitial sites and induce increased strains in the substrate lattice. These high strains can embrittle the substrate material by bringing it closer to its yield stress. Furthermore, when heated during pretreatment or under use, Ar could diffuse and agglomerate into bubbles, introducing porosity and weakening of the interface [19].

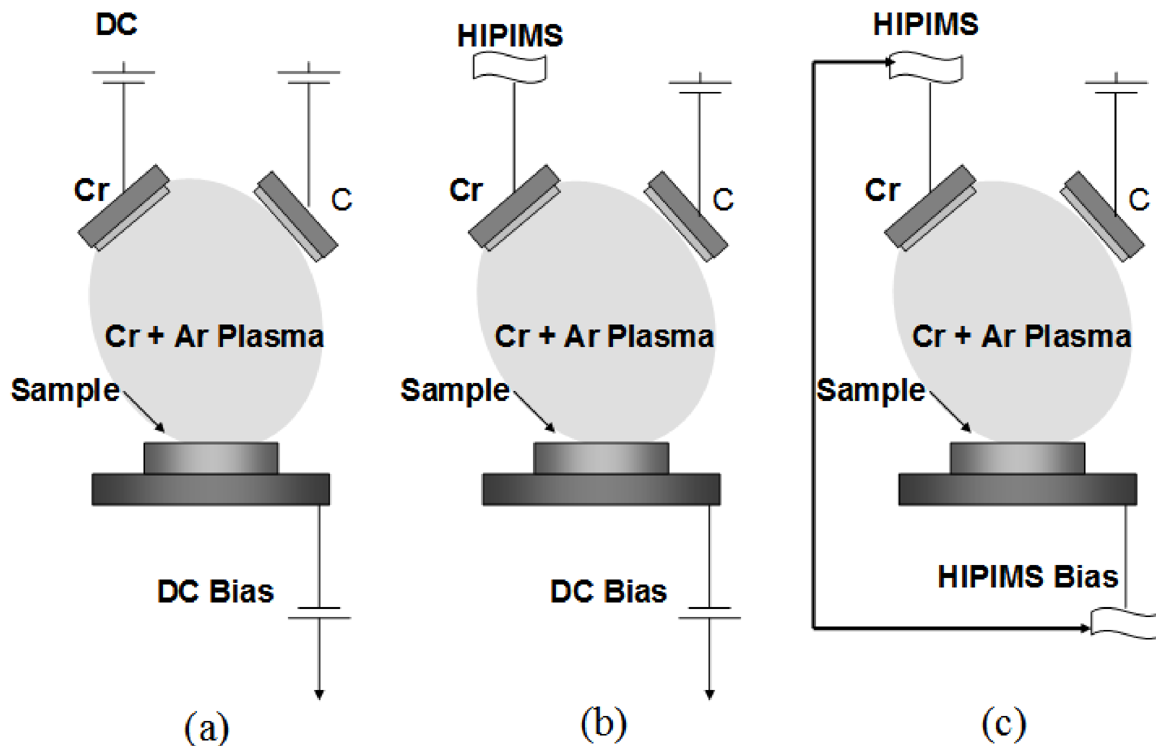

Figure 1: *Different methods to produce plasma cleaning of substrates. (a) Classic process where ions are generated by a magnetron cathode and the bias provided by a negative DC voltage. (b) HIPIMS process, where gas and metal ions are generated by an HIPIMS discharge in the cathode and the bias is provided by a negative DC voltage. (c) Novel process where two HIPIMS power supplies are used in a master-slave configuration whereby the first establishes the discharge in the cathode and the second produces a pulsed substrate bias.*

2.2.2 Sputter Cleaning by gas ions: RF and pulsed-dc substrate biasing

Radio frequency (RF) biasing has been used since the 1970s to induce the energetic particle bombardment of insulating substrates. RF bias supplies, usually operating at 13.56 MHz, are connected to the substrates via a matching network [13].

The use of unipolar pulsed substrate biasing in cathodic arc evaporation was introduced in 1991 by Olbrich *et al* [20] to reduce thermal input associated with

ion bombardment. With the advent of pulsed-DC target sputtering, bias pulsing techniques with frequencies in the range 20-350 kHz become more popular in the late 1990s because it was then realized that it could provide improved control of substrate bombarding ion energy and flux, and be utilized to bias substrates during reactive deposition of insulating films [21]. Unipolar pulsed-DC substrate biasing is often carried out in combination with pulsed-DC target sputtering. In such situations, both target and substrate are usually pulsed at the same frequency (usually 100 kHz) in a synchronous "master-slave" configuration [22-24].

2.2.3 Sputter Cleaning by metal ions: arc technique

An improvement in the adhesion of carbon-based coatings has been the pretreatment in metal arc discharge environment. Bombardment with metal ions is known to provide cleaner interfaces [25]: cathodic arc discharges produce a high flux of metal ions, which bombard the surface of the substrate and remove oxide layers. That was the base for the development in the 1990's of the so-called ABS (Arc Bond Sputtering) technique where a cathodic arc is used to generate metal ions that are accelerated by a DC bias voltage toward the substrate in order to produce an etching prior to the film deposition by magnetron sputtering [26]. As it has been pointed out by many, the multiply ionized metal ions, which are produced in the vapor of the cathodic arc discharge, not only clean the substrate, but also produce low-energy implantation promoting the formation of a graded interface between the substrate and the coating. The formation of such interface provides a relief of film stress, increasing the adhesion of the coatings [27-29].

The effects of DC bias voltage on the composition and structure of the graded interface for enhanced adhesion has been the subject of many studies. For instance, Schönjahn *et al* studied Cr arc etching of M2 mild steel, where an implantation/diffusion layer of Cr in the steel was observed at DC bias voltages of -800 to -1200V [30].

One of the problems of etching with cathodic arc is the production of molten particles which are deposited in the surface to clean. Münz *et al* investigated the generation of droplets by target materials Al, Cu, Ti-Al, Ti, Zr, Cr, Nb, and Mo [31]. They found that the number and size of the droplets depend on the melting point of the metal used during the ion etching, with a typical droplet size of 100 nm.

2.2.4 Sputter Cleaning by metal ions: HIPIMS technique

The metal ion etching by HIPIMS using a DC bias voltage has been first reported by Ehiasarian *et al* [32], as in the scheme shown in Figure 1b. The highly ionized plasma conditions of HIPIMS with 80% metal ions resulted in a more efficient ion bombardment, improving the etching of the substrate and increasing the adhesion of the coatings. It also been shown that the presence of a DC bias voltage promotes the formation of a shallow metal implantation on the surface, promoting the formation of an adherent interface between the substrate and the coating [33].

Recently, the use of high power impulse magnetron sputtering (HIPIMS) technology has been proposed to increase the adhesion of coatings on metal substrates [34]. HIPIMS produces a high flux of ions with high metal content similar to an arc discharge, but without droplets. The ions (gas and metals) are accelerated to the substrate by the use of a DC bias, producing a high rate of substrate etching and also the implantation of metal atoms like in arc discharges.

Helmersson *et al* [29] has reviewed the state of the art for arc and HIPIMS deposition techniques. They pointed out that, while for the DC magnetron sputtering technique, the amount of ionized metal in the plasma is lower than 10%, for the arc and HIPIMS technique that amount can reach 90%. HIPIMS technology also removes the cathodic arc etching droplet problems.

The metal ion etching by HIPIMS using a DC bias voltage has been first reported by Ehiasarian *et al* [32], as in the scheme shown in Figure 1b. The highly ionized plasma conditions of HIPIMS with 80% metal ions resulted in a more efficient ion bombardment, improving the etching of the substrate and

increasing the adhesion of the coatings. It also been shown that the presence of a DC bias voltage promotes the formation of a shallow metal implantation on the surface, promoting the formation of an adherent interface between the substrate and the coating [33].

Different ion metal etching prior to the deposition of coatings have been reported: Cr or Nb for CrN [19, 34, 35] , V for TiAlCN/VCN multilayers [36], Cr for CrAlYN/CrN multilayers [37, 38] , WC for W-DLC and C-DLC multilayers [39], and Cr for DLC and Metal-DLC coatings [40]. Besides our previous work [5-7], to our knowledge there are not reports on the deposition of CN_x (carbon nitride) coatings using the HIPIMS interface sputter cleaning, or on the use of two HIPIMS power supplies for etching (one connected to the cathode and one to the table) [41] .

2.3 New improvements in plasma cleaning and interface formation during PVD processes

The most important problem to solve during the substrate pretreatment by HIPIMS for the cleaning and interface formation is the high current flowing from the cathode to the substrates. In some DC power supplies used for biasing, this high current is interpreted by the bias power supply as the presence of arcing, which causes the power supply to interrupt the operation. This problem has been partially overcome installing large capacitor-resistors banks or special power supplies that can stand the current pulse arriving to the substrates [42, 43]. However, the constancy of the bias during the discharge will depend on the size of the capacitors and resistors. From an industrial point of view, the drawback is that this device occupies a vital space in the chambers, especially if a nearly constant bias voltage is desired.

Based in our innovation [7] we have recently reported initial results for the deposition of highly adherent CN_x films on steel substrates using a novel HIPIMS pretreatment in an industrial production chamber. During the pretreatment, the substrates were pulse-biased in the environment of a HIPIMS Cr plasma in order to sputter clean the surface and to implant Cr^+ metal ions. Subsequently, CN_x

films with superior adhesion to the steel substrates were obtained by DC unbalanced magnetron sputtering.

3. EXPERIMENTAL

The experiments were carried out in a CC-800/9 industrial system manufactured by CemeCon AG in Würselen, Germany. The chamber (85 x 85 x 100 cm) is equipped with four rectangular magnetron sputtering cathodes (50 x 8.8 cm) facing a table holder that can give to the substrates up to three-fold rotation (Figure 2). Due to the nature of our experiments only two out of four cathodes mounted in the system were used. The system is equipped with DC magnetron power supplies Pinnacle 3000 (Advance Energy) and HIPIMS power supplies SINEX 3 (Chemfilt Ionsputtering AB, Linköping, Sweden). The targets materials were Cr and C (99.8% pure). The substrates used in the experiments were Si (100) wafers and SKF3 (AISI 52100) bearing stainless steel.

Cross-sectional specimens for transmission electron microscopy (TEM) investigations were made by gluing slices into Ti disks followed by mechanical polishing and grazing incidence (4º) Ar^+ ion thinning at 10 kV to electron transparency using a Technoorg Linda IV6 ion milling unit. The ion energy was decreased in the final period of the ion milling procedure down to 500 eV to decrease the ion damage. The high-resolution TEM (HRTEM) investigations were made in a Technai G2 and a JEOL 3010 electron microscope operated at 200 and 300 kV, respectively. EDS line scans were recorded in the Technai G2 microscope.

3.1 Substrate Pretreatment and Coating

The metal substrates were mirror polished by mechanical polishing with a sequence of 6, 3, and 1 μm diamond pastes, and then were cleaned using a sequence of ultrasonic washing stages with alkaline detergents (Decon-90 at

5%), de-ionized water rinsing and air-drying. Prior to loading into the chamber, all the substrates were ultrasonic cleaned with acetone and isopropanol, and blow-drying with nitrogen gas.

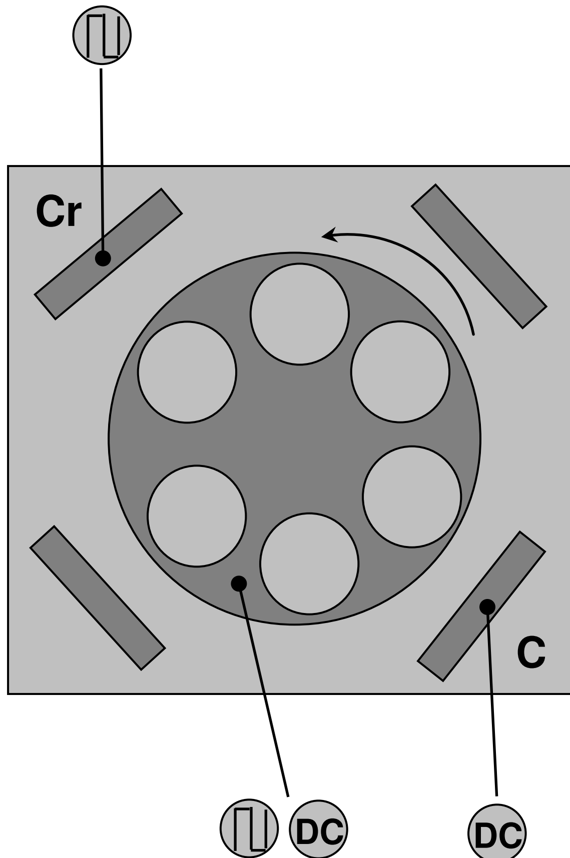

Figure 2: *Schematic configuration of the chamber, showing four magnetron sputtering cathodes and the table holder that can give to the substrates up to three-fold rotation. In our experiments we have used two cathodes and a single rotation of the substrates.*

Different substrate pre-treatments were carried out prior to the deposition of the CN_x films (see Figure 1):

(a) A first group of substrates (Figure 1 a) were biased to a DC voltage of –1200 V while the Cr target was operated in a DC mode at a pressure of 3 mTorr of Ar and a current of 1 A during 30 minutes;

(b) A second group of substrates (Figure 1 b) were biased to a DC voltage of -600 V while a HIPIMS source was operated at a pressure of 3 mTorr, with a

peak target voltage of 1100 V, a frequency of 150 Hz, and a pulse width of 100 μs, during 30 minutes;

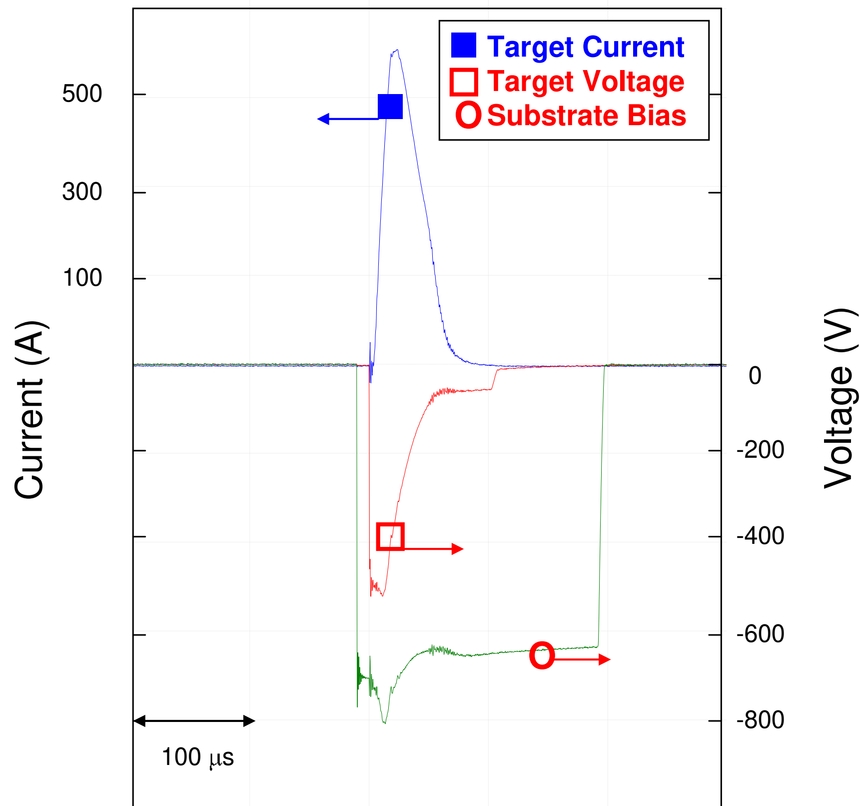

Figure 3: *Target current (■), target voltage (□) and bias voltage (○) waveforms recorded in one of the experiments of the configuration illustrated in Figure 1c.*

(c) The third group of substrates (Figure 1 c) were biased to a HIPIMS source with peak voltages of in the range 400-800 V, a frequency of 150 Hz, and a pulse width of 200 μs. The target was also connected to a second HIPIMS source operated at a pressure of 3 mTorr, with a peak target voltage in the range 500-1100 V, a frequency of 150 Hz, and a pulse width of 100 μs, during 30 minutes. Both HIPIMS power supplies were synchronized, being the one in the target the "master" and the one in the substrate the "slave". The voltage pulse in the target was programmed to start 10 μs after the pulse in the substrate in order to assure the stability of the bias voltage (Figure 3).

The coating step was carried out by DC magnetron sputtering of a C target in a reactive atmosphere of Ar and N_2 (partial pressure ratio of 84:16 and total pressure of 3 mTorr), target power of 1800 W, and a negative bias voltage of 25 V.

No heating treatment was used during the pretreatment or the deposition steps.

3.2 Cathode Current and Plasma Characterization

The target current was measured with a Tektronix CT-04 high current transformer together with a Tektronix TCP202 current probe mounted right at the connection to the vacuum chamber. A Tektronix P6015 high voltage probe was used to measure the cathode voltage. Current and voltage waveforms were recorded with the Picoscope 3000 real time digital storage PC oscilloscope from Pico Technology.

The optical emission from the plasma was measured in the light-of-sight geometry through a port window of the chamber and the probe was directed towards the race track. A spectrometer (Mechelle Sensicam 900) connected to a collimator via an optical fiber was used to record the emission from the plasma. The spectral range of the spectrometer was 300-1100 nm. The optical emission spectra were acquired at argon gas pressures ranging between 0.5 and 10 mTorr and for different target voltages (implying different peak power levels). The shutter speed of the spectrometer was set to 100 ms, meaning that all data were time-averaged over ca. 30 pulses (the pulsing frequency was fixed at 300 Hz).

3.3 Adhesion Tests

Two methods were used to test the adhesion. The Daimler-Benz Rockwell-C adhesion test, developed by the Union of German Engineers (Verein Deutscher Ingenieure, VDI [44]) uses a standard Rockwell hardness tester fitted with a Rockwell C-type diamond cone indenter with an applied load of 150 kg. The result is obtained by using an optical microscope and classifying the adhesion as

HF 1 to HF 6 according to the level of cracking or coating delamination around the indent. Only indents classified as HF 1 and HF 2 correspond to adequate adhesion [45].

The scratch test (REVETEST, CSM) has also been applied to determine the adhesive strength of the coatings. A Rockwell C diamond was used to scratch the surface of the coated samples at a constant speed and under a continuously increasing load. The critical load where the coating start to fail was detected by means of an acoustic sensor and compared with observations from a built-in video microscope. A sliding velocity of 10 mm/min and scratch length of 12 mm were used in all the tests.

4. RESULTS AND DISCUSSION

4.1 Target Current-voltage-time Characteristics

The target current and voltage responses were studied at different output voltages of the power supply. The chamber was evacuated to the base pressure of 10^{-5} Torr. Argon of purity 99.9997% was introduced through a leak valve to start and maintain the discharge. The Cr cathode was operated by a HIPIMS power supply capable of delivering 2 kV peak voltage pulses and the average power of up to 10 kW. In the case of industrial size targets, like the ones used in this experiment, the exact shape of current and voltage waveforms is to a large extent determined by the capacitor bank used in the powering unit [46]. As can be seen in Figure 4, the voltage is not constant throughout the pulse in the present set up, but rather drops from the peak value reached right at the beginning of the pulse (before any current flows) as the charge is withdrawn from the capacitor bank after the ignition of the discharge. The resulting target current is thus proportional to the rate at which voltage drops at the target according to $I = C \times dU/dt$, where C stands for capacitance, I and U are target current and target voltage. As soon as the target voltage becomes too low to sustain discharge, current goes down to zero limiting the power pulse to about 80 µs. In

this way the target area sets the limit for duration of the current (and power) pulses. It can also be seen from the data in Figure 4 that as soon as the peak target voltage increases above 850-900 V the current peaks consists of two components. The bigger peak in the left is generated by Ar^+ ions and the smaller peak in the right is related to Cr^+ ions. According to previous reports, the separation of the peaks can be related to the delay in the generation of Cr^+ ions for high power discharges [47, 48].

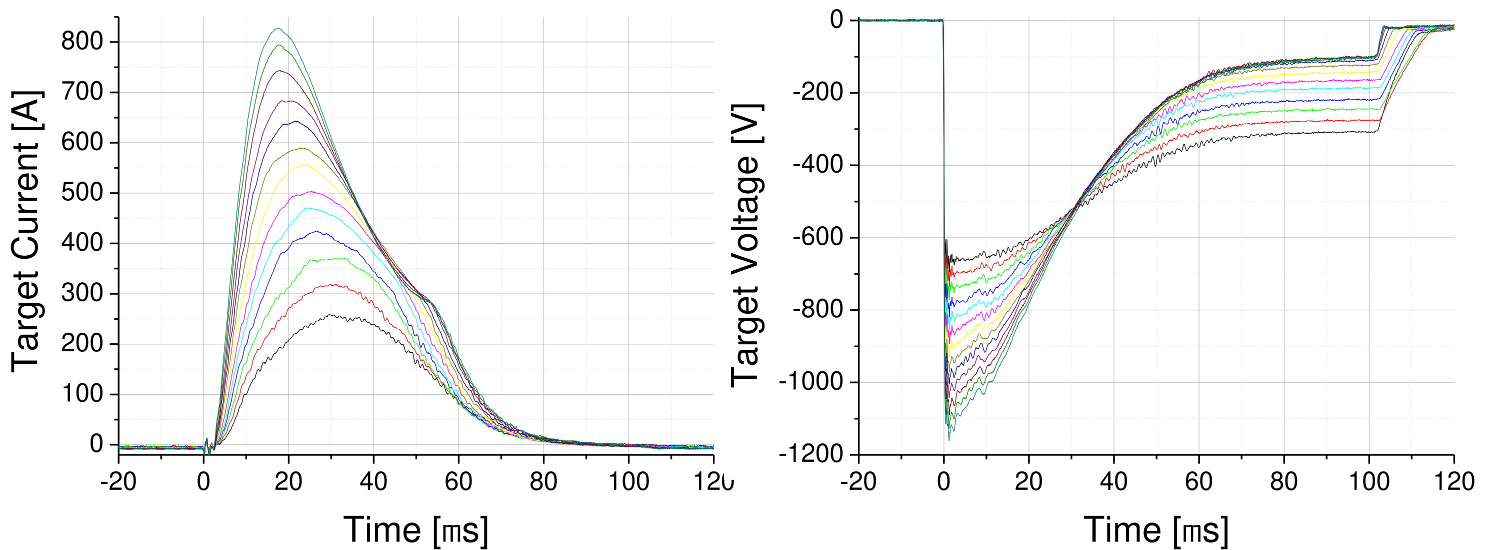

Figure 4: *Target current (top) and target voltage (bottom) waveforms recorded at 3 mTorr argon gas pressure. The parameter that is varied here is the output voltage of the power supply, what has an effect on the peak value of the target voltage and, in consequence, on the peak target current. The energy density (per pulse) indicated in the legend box is basically the product of current and voltage traces integrated over the time period of one pulse (100 µs) and divided by the whole area of the target.*

4.2 Plasma Chemistry during Pre-treatment

The chemistry of the ion flux during the HIPIMS pretreatment was studied by optical emission at different energies and pressure conditions. In Figure 5a the optical emission intensities of the strongest lines, corrected for transition probabilities according to the method proposed in refs. [49, 50], are plotted for

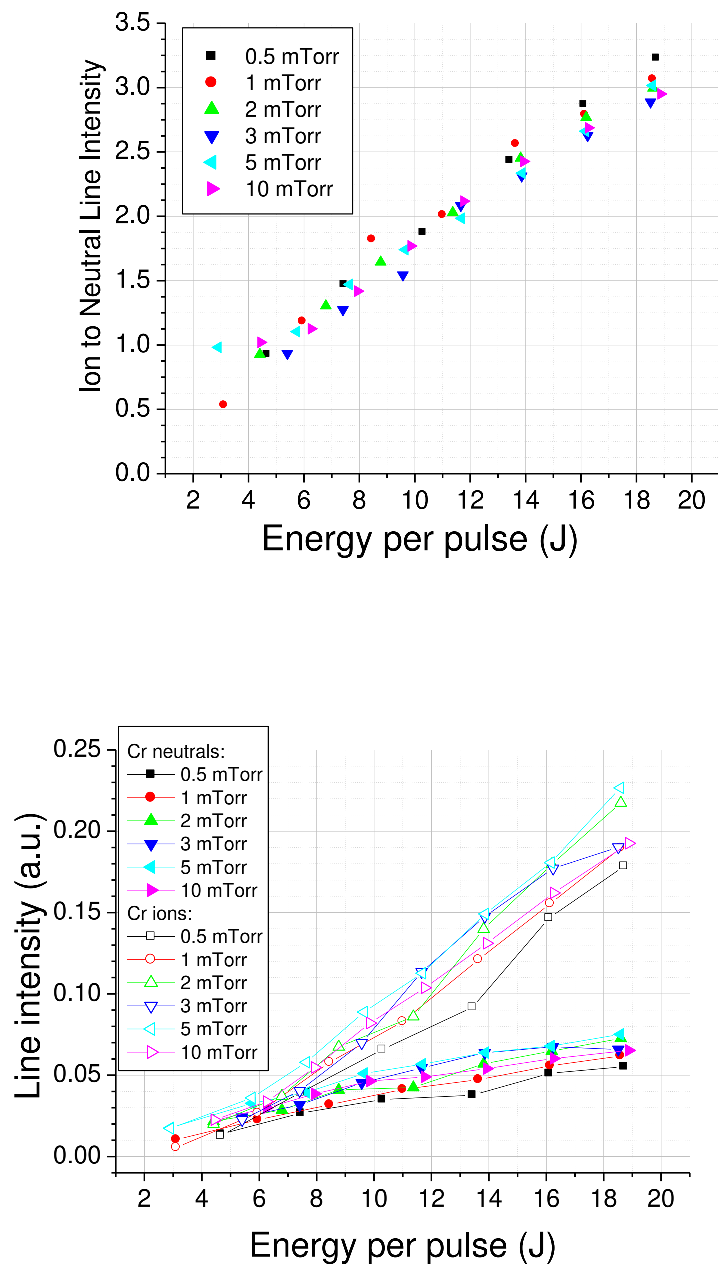

Figure 5: *a) The dependence of emission intensity from Cr-I (399.1 nm) and Cr-II (336.8 nm) lines on the energy density per pulse. b) The dependence of ion-to-neutral intensity ratio as a function of energy density per pulse. The working gas pressure was varied between 0.5 mTorr and 10 mTorr. In order to facilitate comparison line intensities are corrected for transition probability of the spontaneous emission (A) and the upper level degeneracy (g).*

Cr^+ ions and Cr neutrals, respectively, versus energy per pulse for various argon gas pressures. The emission lines chosen for comparison are Cr-I at 399.2 nm and Cr-II at 336.9 nm. It is clearly observed that there is a linear relation between the intensity of optical emission of both Cr^+ ions and Cr neutrals and the energy per pulse. Especially, the slope of the linear function for Cr^+ ions is much larger than that of Cr neutrals. The emission intensity from Cr^+ ions increases roughly by a factor of eight, whereas the signal from Cr neutrals increases only about three times as the peak voltage on the cathode doubles (from 600 V to 1200 V). Since the excitation energy in both cases is close to each other, one can conclude qualitatively that the relative amount of Cr^+ ions with respect to Cr atoms increases significantly with increasing energy per pulse (Figure 5b). This trend is more or less independent of the working gas pressure. The detail quantification of the optical emission spectra is, however, complicated due to the dynamic nature of the discharge, lack of thermodynamic equilibrium (unknown electron temperature), and experimental setup (line-of-sight geometry), etc.

4.3 Interface Characterization

The microstructure of the interface between CN_x films and steel substrates was studied by cross-sectional TEM in samples deposited with the HIPIMS biased substrate method of Figure 1c. Figure 6 shows the formation of a modified Cr layer between the steel substrate and the CN_x film prepared by this method. The layer is characterized by a polycrystalline structure of approximately 100 nm. The transition between the substrate and the modified layer, which appears to have more contrast, was also analyzed by HRTEM (Figure 7). A ~5 nm amorphous transition layer is visible between the Cr and the steel. The overall structure of the interface is dense, with no formation of bubbles or voids, pointing to a strong bonding between the steel substrate and the CN_x coating.

The modified layer is formed during the pretreatment stage where Ar^+ and Cr^+ ions generated by the HIPIMS discharge on the Cr target bombard the substrate biased by the second HIPIMS power supply. Two counteracting processes compete during the formation of the polycrystalline layer:

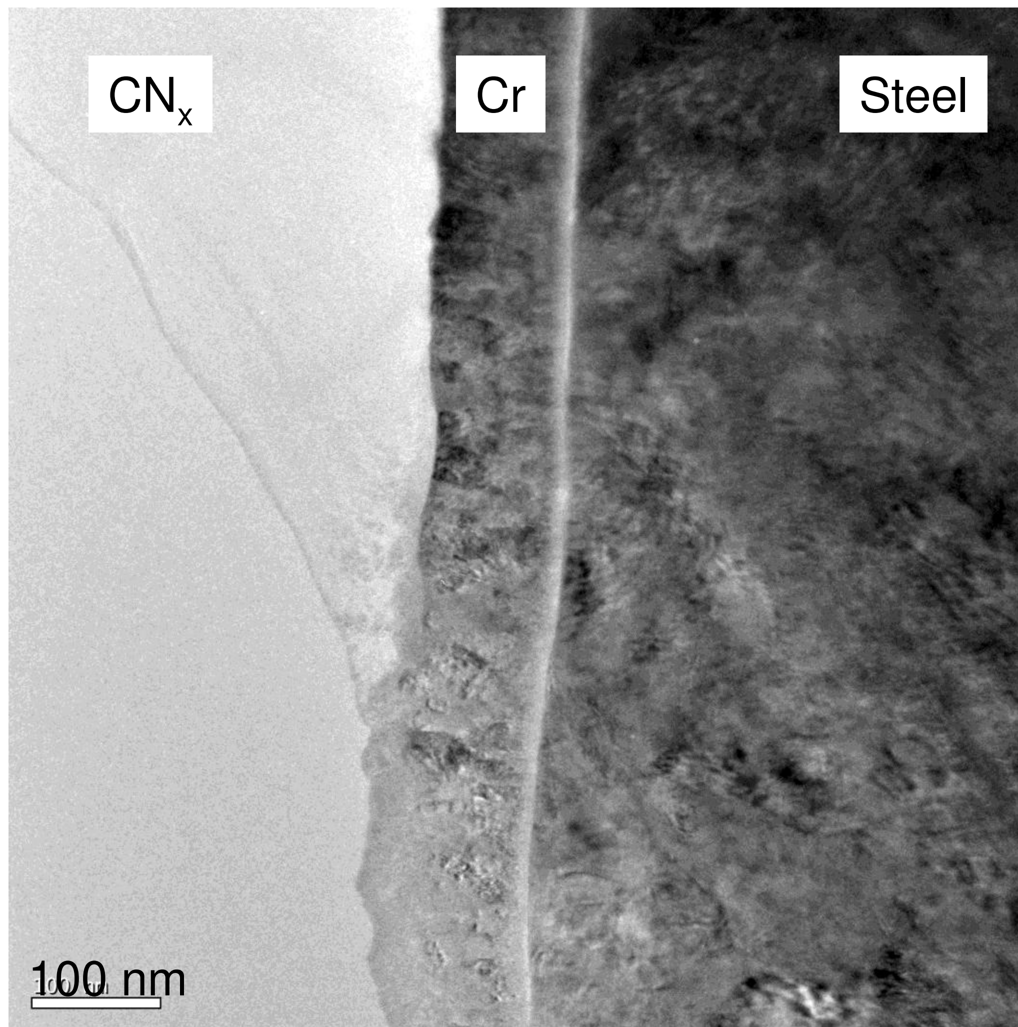

Figure 6: *Cross-sectional TEM image showing the CN_x/steel interface. A polycrystalline Cr microstructure of about 100 nm thick is observed.*

- the Cr concentration decreases due to sputter removal.
- the Cr concentration increases due to condensation on the surface.

The effective sputter removal effect of Ar^+ + Cr^+ ions bombardment was evaluated by a simple experiment on two Si(100) substrates using the configuration of Figure 1c. The Cr target was operated during 30 minutes at a pressure of 3 mT of Ar, with a peak target voltage of 1100 V, a frequency of 150 Hz, and a pulse width of 100 μs. These conditions are similar to the sample shown in Figure 6, however, one of the Si substrates had a floating bias. After

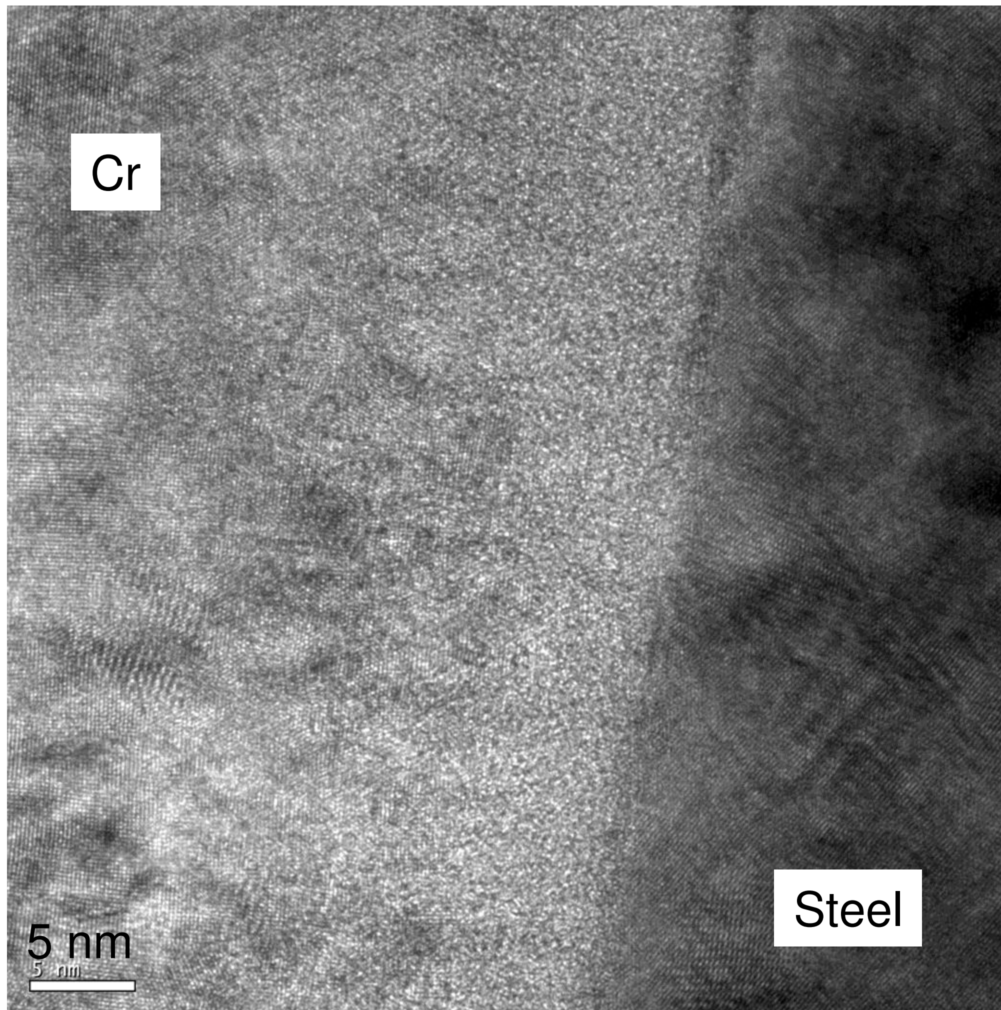

Figure 7: *Cross-sectional HRTEM image of the higher contrast region shown in Figure 6. A ~ 5nm amorphous transition layer can be seen between the polycrystalline Cr and the steel.*

the experiment, cross-sectional SEM observations of the Si substrates revealed a Cr layer of 1.2 μm thickness for the substrate held at floating bias, in contrast to the 0.1 μm of the biased sample grown under HIPIMS Ar^+ + Cr^+ ion bombardment.

The chemical composition of the amorphous transition layer was studied in more detail by TEM-EDS. Fig 8 shows a 40 nm line scan across the interface between the Cr layer and the steel substrate, with a ~ 5 nm thick layer of mixed Cr and Fe, which probably corresponds to the dark layer visible in Figures 6 and

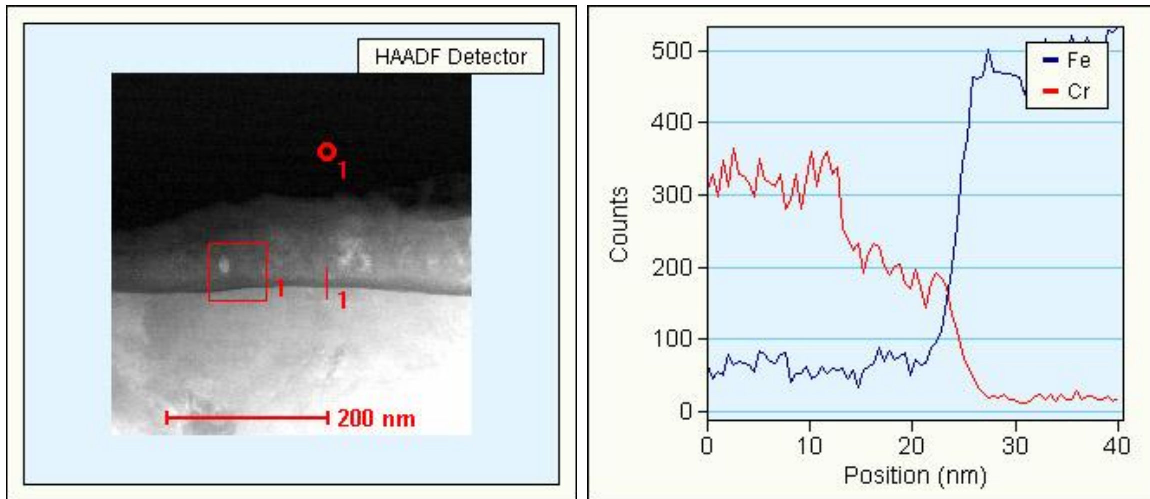

Figure 8*: Line-scan TEM-EDS chemical composition analysis of the transitional amorphous layer shown in Figure 7.*

7. Oxygen was not detected in the sample. It appears that native steel oxides were effectively sputtered cleaned of the surface providing a clean contact between substrate and coating. The presence of this mixed amorphous interface can be explained by the magnitude and composition of the ion flux. The introduction of Cr into the substrate is initiated by the direct physical implantation of Cr extracted from the plasma and accelerated by the high bias voltage. Additionally, the retention of Cr is facilitated by the high affinity of the metal ion, which could be incorporated at lattice sites of the substrate. In the system Cr-Fe there is a complete thermodynamic solubility and there is not limit to the expected concentration that can be incorporated [19, 35, 51]. Recently, Ehiasarian *et al* [19] have simulated the depth of Cr incorporation resulting from implantation using the TRYDYN code. Assuming a steel substrate and bombarding ion flux concentration of 50 at. % Cr^{3+}, 30% at % Cr^{4+} and 20 at. % Ar^{1+}, he obtained maximum range of implantation of 7 nm for a DC bias voltage of 600 V. The calculated ion range is similar to the incorporation depth profile of Cr measured by our TEM-EDS (figure 8). This result contrasts with the ones from other authors [19, 35, 52] where a mixed interface of 15-20 nm has been observed. The difference can be associated to thermal diffusion of Cr into the

substrate. While these authors have been using substrate temperatures in the range 250-500 C, our samples have been deposited at room temperature. It is well known that during DC bias cleaning of the substrates the surface temperature increases. In our case, we know the maximum substrate temperature during the dual-HIPIMS plasma etching (Figure 1c) was below 200 ^{0}C because we did not observe a change in the HV hardness of our SKF3 steel substrates [53].

We could not analyze the interface of samples deposited by the other two methods (Fig 1a and 1b) because the adhesion of the film to the substrate was too weak to support the sample preparation technique. In some cases, most of the coatings area delaminated as soon as the samples were exposed to air.

Cross-sectional and plan-view SEM images of the CN_x films (Figure 9) have revealed a coating with a dense microstructure, similar to that observed in amorphous CN_x films deposited in laboratory-scale chambers [1, 54].

4.4 Adhesion Tests

Figure 10 illustrates typical results from the Rockwell-C tests on samples deposited by the three different substrate pretreatment methods of Figure 1. When the samples were biased to a DC voltage of – 1200 V and the Cr target was operated in a DC mode, the resulting indentation (Fig. 10a) can be identified as the adhesion strength quality HF5. The CN_x coating shows radial cracks and large delaminations around the crater caused by the piling up of the substrate, which can be related to the poor adhesion of the film to the substrate. Figure 10b shows the resulting indentation of coatings when the samples were biased to a DC voltage of -600 V while the Cr target was operated with a HIPIMS source. In this case the CN_x coating has a typical failure that can be related to the adhesion strength quality HF3: fine cracks in the indentation area with small delamination in the vicinity of the crater. Figure 10c shows no visible failures around the indentation crater, and can be classified as adhesion strength quality HF1. This excellent adhesion was obtained when both substrate bias and Cr target were connected to two synchronized HIPIMS power supplies, as shown in Figure 1c.

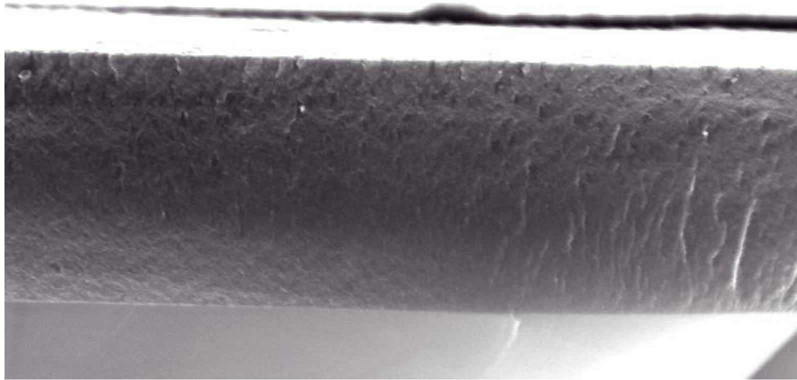

Figure 9: *Cross-sectional (a) and plan-view (b) SEM image of the CN_x film. A dense microstructure is observed.*

Figure 11 shows typical scratch test results from samples deposited with the plasma pretreatment methods shown in Figure 1. In these experiments, the minimum load of the scratch tester was 10 N and the maximum load was 50 N. The critical load where the films failed is different in each case, and the results agree with the adhesion measurements done by the Rockwell-C adhesion test (Figure 10):

a) When gas ions are generated by a magnetron cathode and 1200 V bias is provided by a negative DC voltage, like in Figure 1a, the critical load to start detaching the film is very low, about 7 N. A significant spallation of the CN_x film observed both, inside and outside of the scratch track, can be related to the weak adhesion of the film to the substrate (Figure 11a).

b) When the gas and metal ions are generated by an HIPIMS discharge in the cathode and the bias is provided by a negative DC voltage, like in Figure 1b, the critical load is 48 N. The micrograph of Figure 11b shows a typical buckling failure in the form of curved cracks and patches extending to the edges of the scratch track. The failure occurs in response to the compressive stresses generated ahead of the moving indenter [55]. Localized regions containing interfacial defects allowed the coating to buckle in response to the stresses generated by the indenter before the critical load was reached.

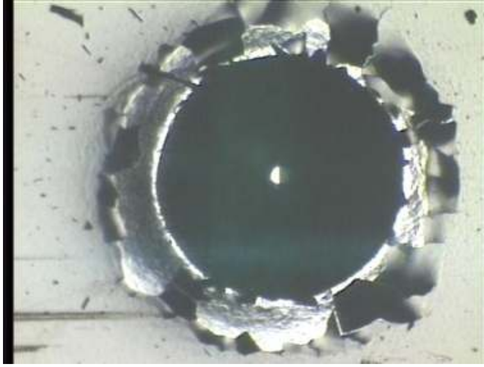

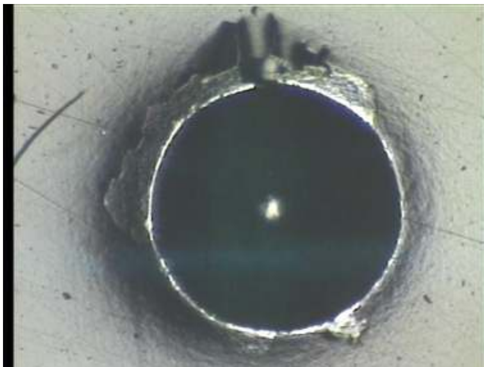

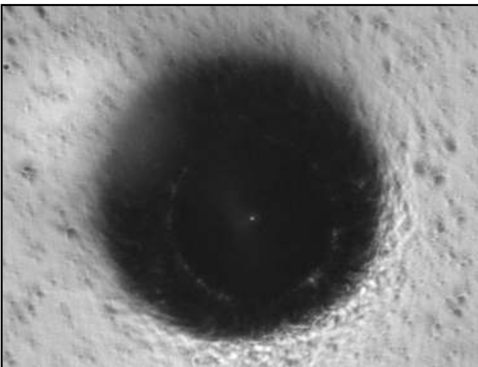

Figure 10*: Adhesion strength HF of CN_x films deposited by DC magnetron sputtering. Each optical micrograph represents a sample deposited with different substrate plasma pretreatment (a) HF = 6, when gas ions are generated by a magnetron cathode and the bias is provided by a negative DC voltage, like in Figure 1a. (b) HF = 3, when the gas and metal ions are generated by an HIPIMS discharge in the cathode and the bias is provided by a negative DC voltage, like in Figure 1b. (c) HF = 1 when two HIPIMS power supplies are used in a master-slave configuration, like in Figure 1c.*

c) When two HIPIMS power supplies are used in a master-slave configuration, like in Figure 1c, the critical load is higher than 50 N. No adhesion failures are observed inside or outside the track, demonstrating an excellent adhesion coating-substrate (Fig 11c). Scratch test experiments with maximum loads of 100 N showed that the critical load in this case is 84 N.

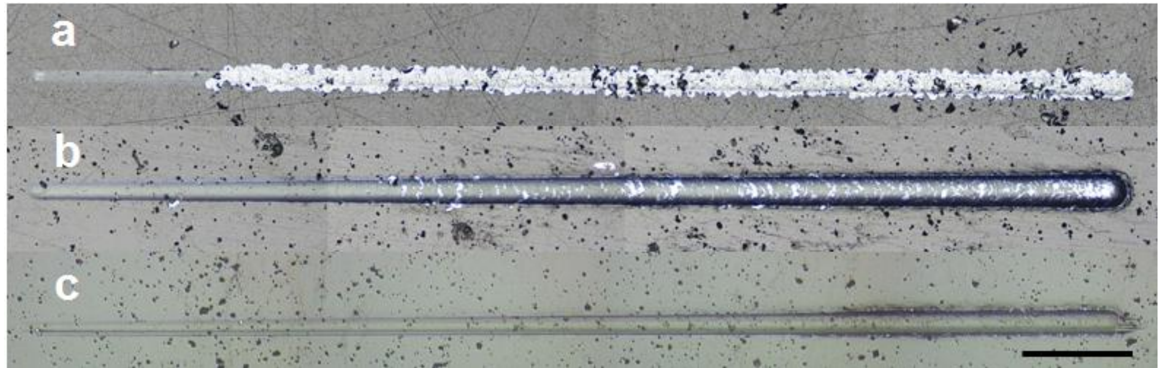

Figure 11*: Optical micrographs of scratch tracks for CN_x films deposited by DC magnetron sputtering. Each picture represents samples deposited with different substrate plasma pretreatment (a) critical load of 16 N, when gas ions are generated by a magnetron cathode and the bias is provided by a negative DC voltage, like in Figure 1a; (b) critical load of 44 N, when the gas and metal ions are generated by an HIPIMS discharge in the cathode and the bias is provided by a negative DC voltage, like in Figure 1b; (c) critical load higher than 50 N, when two HIPIMS power supplies are used in a master-slave configuration, like in Figure 1c. The length of the scale bar is 0.4 mm, which corresponds to 4 N.*

We have also investigated the effect of substrate bias voltage and Cr target voltage on the adhesion of CN_x films deposited by the pretreatment illustrated in Figure 1c. The adhesion map of Figure 12 shows that there is a process parameter area centered at 600 V substrate bias voltage and 1100 V target voltage where the adhesion strength quality is excellent, namely HF1-HF2. Outside of this area the resulting adhesion strength quality is HF5-HF6.

At the optimum conditions of 1100 V Cr cathode voltage and 600 V bias voltage, a gradual interface between Cr and steel is formed (Figures 6-8) that can withstand the high stresses of the CN_x films. As we have discussed in Section 4.3, at the beginning of the plasma treatment, the Ar^+ + Cr^+ ion

bombardment have enough time to clean the substrate from oxides and other contaminants, and tends to sputter away the exposed steel substrate and implant Cr ions. As a result, the film adhesion with an optimal intermixing at the interface becomes very strong, with high critical loads in the scratch test (Figure 11).

We can understand the effect of varying the HIPIMS pretreatment cathode voltage on the results shown in the adhesion map of Figure 12. At cathode voltages higher than 1100 V, Cr deposition will be much faster than Ar^+ + Cr^+ ion sputtering. If the rate of Cr deposition is very high, the substrate will be quickly covered with a (thin) Cr film, little or no Cr-substrate intermixing will be induced and the interface will be sharp: the film adhesion will be poor. At cathode voltages below 1100 V, the resulting rate of Cr deposition on the substrate could be very low due to the Ar^+ + Cr^+ ion sputtering. The Cr will not form a uniform layer over all the surface of the substrate, leaving uncovered parts of the steel substrate. Little or no Cr-substrate intermixing will be induced and the interface will be sharp: the film adhesion will be poor.

The effect of the HIPIMS pretreatment bias substrate on the results shown in Figure 12 can also been explained. At bias voltages above 600 V, the strong Ar^+ + Cr^+ ion sputtering creates defects on the substrate, and could lead to Ar entrapment on the interface (*c.f.* section 2.2.1), leading to a poor film adhesion. At bias voltages below 600 V, the resulting sputter etching rate would be not enough to clean the substrate from oxides and other contaminants, and/or there is not enough energy to implant Cr ions and form the amorphous transition layer. As a result, the film adhesion will be also poor.

5. CONCLUSIONS

Carbon nitride films were deposited onto SKF3 (AISI 52100) bearing stainless steel substrates in an industrial chamber by DC magnetron sputtering with various interfacial treatments. A novel HIPIMS pretreatment is presented where two HIPIMS power supplies are used in a master-slave configuration: one establishes the discharge in the cathode and the second produces a pulsed substrate bias. This configuration provides a more stable bias voltage during

HIPIMS plasma pretreatment and is an alternative way to achieve excellent results without the use of specially designed DC power supplies.

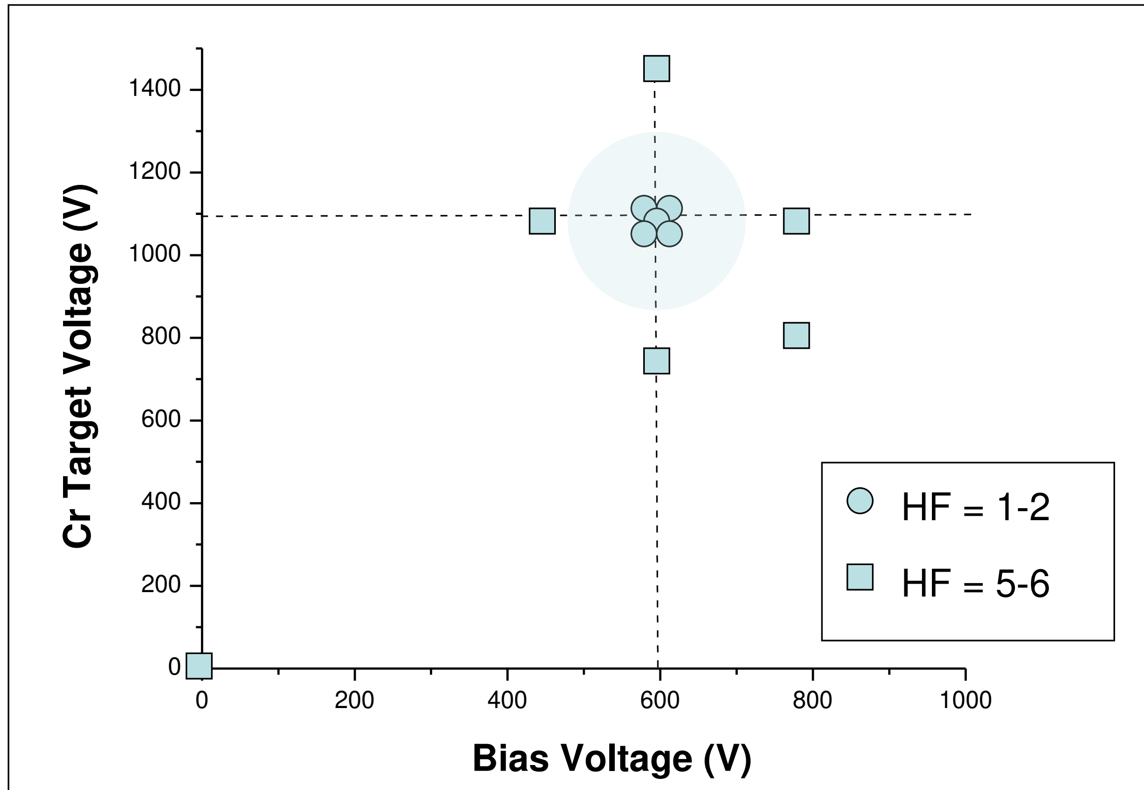

***Figure 12**: Adhesion map of CN_x films deposited by DC magnetron sputtering with different HIPPIMS bias treatment. The plasma pretreatment has been done using two HIPIMS power supplies, as indicated in Figure 1c. The x-axis represents the investigated bias voltage and the y-axis the applied Cr target voltage. The shadowed area represents the optimal conditions where the samples have an adhesion strength HF equal to 1 or 2. The sample deposited with zero bias and target voltages is a sample without plasma treatment.*

Adhesion of CN_x films evaluated by the Daimler-Benz Rockwell-C and the scratch tests was remarkably increased to maximum value by our deviced pretreatment through the formation of an optimal interfacial mixing layer of Cr and steel.

We demonstrate for first time the deposition of thick (1-3 μm) adherent CN_x coatings on steel substrates in an industrial scale chamber, opening the

possibility for new tribological applications of carbon nitride films. The findings of this study are also expected to be of general validity and applicability in the industrial scale deposition of carbon-based and other coating materials.

6. ACKNOWLEDGMENTS

The support from the Swedish Governmental Agency for Innovation Systems (VINNOVA) and the Swedish Foundation for Strategic Research (SSF) are greatly appreciated. Ms. Biljana Mesic from CemeCon AG is acknowledged for assistance during the tribological characterization of the coatings.

REFERENCES

1. **E. Broitman, J. Neidhardt, and L. Hultman, in *Tribology of Diamond-Like Carbon Films : Fundamentals and Applications*, C. Donnet and A. Erdemir, Editors. 2007, Springer: N. York. p. 620-653.**
2. **E. Broitman, G.K. Gueorguiev, A. Furlan, N.T. Son, A.J. Gellman, S. Stafström, and L. Hultman. Thin Solid Films, 2008. 517(3): p. 1106-1110.**
3. **E. Broitman, V.V. Pushkarev, A.J. Gellman, J. Neidhardt, A. Furlan, and L. Hultman. Thin Solid Films, 2006. 513(3): p. 979-983.**
4. **E. Broitman, W.T. Zheng, H. Sjostrom, I. Ivanov, J.E. Greene, and J.E. Sundgren. Applied Physics Letters, 1998. 72(20): p. 2532-2534.**
5. **E. Broitman, Z. Czigány, R. Cremer, X. Zhou, and L. Hultman. in *Book of Abstracts - 36th International Conference on Metallurgical Coatings and Thin Films*. 2009. San Diego (CA): p. 75-76.**
6. **E. Broitman, G. Greczynski, J. Bohlmark, M. Alunovic, R. Cremer, and L. Hultman. in *Book of Abstracts - 35th International Conference on Metallurgical Coatings and Thin Films*. 2008. San Diego (CA): p. 108.**
7. **E. Broitman, L. Hultman, and R. Cremer, *"Beschichtungsverfahren und Vorrichtung zum Beschichten" (Coating process and device for coating)* 2008: Germany - Patent # DE102008021912A1 Date: 05.11.2009.**
8. **N. Bertrand, B. Drevillon, A. Gheorghiu, C. Senemaud, L. Martinu, and J.E. Klemberg-Sapieha. Journal of Vacuum Science & Technology A: Vacuum, Surfaces, and Films, 1998. 16(1): p. 6-12.**
9. **B.N. Chapman. Journal of Vacuum Science and Technology, 1974. 11(1): p. 106-113.**
10. **D.M. Mattox. 2003, William Andrew Inc. Publishers: New York. p. 34-36.**
11. **D.M. Mattox, in *"Handbook of Vacuum Technology"*, D.M. Hoffman, B. Sing, and J.H. Thomas, Editors. 1998, Academic Press: New York . Chapter 4.9.**
12. **J. Strong. Review of Scientific Instruments, 1935. 6: p. 97.**
13. **R.F. Bunshah,*Handbook of Deposition Technologies for Films and Coatings*. ed. R.F. Bunshah. 1995, N. York: Noyes Publications. 117-120.**
14. **J.E.E. Baglin, in *Fundamentals of Adhesion*, L.-H. Lee, Editor. 1991, Springer: New York. p. 363.**
15. **H.E. Farnsworth, R.E. Schlier, T.H. George, and R.M. Burger. Journal of Applied Physics, 1955. 26(2): p. 252-253.**
16. **D.M. Mattox. Electrochemical Technology, 1965. 2: p. 295.**
17. **M. Ohring,*"The Materials Science of Thin Films"*. 1992, New York: Academic Press. 129-131.**
18. **A. Anders. Surface and Coatings Technology, 2005. 200(5-6): p. 1893-1906.**
19. **A.P. Ehiasarian, J.G. Wen, and I. Petrov. Journal of Applied Physics, 2007. 101(5): p. 054301-10.**
20. **W. Olbrich, J. Fessman, G. Kampschulte, and J. Ebberink. Surf. Coat. Technol., 1991. 49: p. 258-262.**
21. **M. Audronis, A. Matthews, and A. Leyland. Journal of Physics D: Applied Physics, 2008. 3: p. 035309.**

22. **R.D. Arnell, P.J. Kelly, and J.W. Bradley. Surface & Coatings Technology, 2004. 188-189: p. 158-163.**
23. **A. Anders. 2003.**
24. **K.E. Cooke, J. Hamsphire, W. Southall, and D.G. Teer. Surface and Coatings Technology, 2004. 177-178: p. 789-794.**
25. **G. Håkansson, L. Hultman, J.E. Sundgren, J.E. Greene, and W.D. Münz. Surface and Coatings Technology, 1991. 48(1): p. 51-67.**
26. **W.D. Münz, D. Schulze, and F.J.M. Hauzer. Surface and Coatings Technology, 1992. 50(2): p. 169-178.**
27. **A. Anders. Vacuum, 2002. 67(3-4): p. 673-686.**
28. **I.G. Brown. Annu. Rev. Mater. Sci., 1998. 28: p. 243-269.**
29. **U. Helmersson, M. Lattemann, J. Bohlmark, A.P. Ehiasarian, and J.T. Gudmundsson. Thin Solid Films, 2006. 513(1-2): p. 1-24.**
30. **C. Schonjahn, A.P. Ehiasarian, D.B. Lewis, R. New, W.D. Munz, R.D. Twesten, and I. Petrov. in. 2001: AVS.**
31. **W.D. Münz, I.J. Smith, D.B. Lewis, and S. Creasey. Vacuum, 1997. 48(5): p. 473-481.**
32. **A.P. Ehiasarian, W.D. Münz, L. Hultman, U. Helmersson, and I. Petrov. Surface and Coatings Technology, 2003. 163-164: p. 267-272.**
33. **A.P. Ehiasarian, P.E. Hovsepian, L. Hultman, and U. Helmersson. Thin Solid Films, 2004. 457(2): p. 270-277.**
34. **W.D. Münz. Vakuum in Forschung und Praxis, 2008. 20(S1): p. 27-32.**
35. **M. Lattemann, A.P. Ehiasarian, J. Bohlmark, P.Å.O. Persson, and U. Helmersson. Surface and Coatings Technology, 2006. 200(22-23): p. 6495-6499.**
36. **P.E. Hovsepian, A.P. Ehiasarian, A. Deeming, and C. Schimpf. Vacuum, 2008. 82(11): p. 1312-1317.**
37. **P.E. Hovsepian, A.P. Ehiasarian, and U. Ratayski. Surface and Coatings Technology, 2009. 203(9): p. 1237-1243.**
38. **P.E. Hovsepian, C. Reinhard, and A.P. Ehiasarian. Surface and Coatings Technology, 2006. 201(7): p. 4105-4110.**
39. **W.D. Munz, M. Schenkel, S. Kunkel, J. Paulitsch, and K. Bewilogua. Journal of Physics: Conference Series, 2008. 100(8): p. 082001.**
40. **L.A. Donohue, A. Torosyan, P. May, D.E. Wolfe, J. Kulik, and T.J. Eden. Plating & Surface Finishing, 2009(March): p. 38-46.**
41. ***Databases used for research of scientific publications: SciFinder, Web of Science, and Google Scholar.***
42. ***Bias power supply type BP12 manufactured by Huettinger Electronic***
43. **A.P. Ehiasarian, R. Tietema, P.E. Hovsepian, and D. Doerwald, *Vacuum treatment apparatus with additional voltage supply - Patent Application GB20060007269 20060411*. 2007, Hauzer Techno Coating BV (NL); Univ Sheffield Hallam (GB): United Kingdom.**
44. **Verein-Deutscher-Ingenieure,*Daimler Benz Adhesion Test, VDI 3198*. 1992, Dusseldorf: VDI-Verlag. p. 7.**
45. **N. Vidakis, A. Antoniadis, and N. Bilalis. Journal of Materials Processing Technology, 2003. 143-144: p. 481-485.**

46. **J. Böhlmark, *Fundamentals of High Power Impulse Magnetron Sputtering*, in *Department of Physics, Chemistry and Biology (IFM)*. 2006, Linköping University, Ph.D. Dissetation Nr. 1014. p. 64.**
47. **A.P. Ehiasarian, R. New, W.D. Münz, L. Hultman, U. Helmersson, and V. Kouznetsov. Vacuum, 2002. 65(2): p. 147-154.**
48. **A. Vetushka and A.P. Ehiasarian. Journal of Physics D: Applied Physics, 2008. 41: p. 015204.**
49. **C. Christou and Z.H. Barber. Journal of Vacuum Science & Technology A: Vacuum, Surfaces, and Films, 2000. 18(6): p. 2897-2907.**
50. **J. Bohlmark, J. Alami, C. Christou, A.P. Ehiasarian, and U. Helmersson. Journal of Vacuum Science & Technology A: Vacuum, Surfaces, and Films, 2005. 23(1): p. 18-22.**
51. **F. Bergner, A. Ulbricht, and C. Heintze. Scripta Materialia, 2009. 61(11): p. 1060-1063.**
52. **A.P. Ehiasarian, A. Anders, and I. Petrov. Journal of Vacuum Science & Technology A: Vacuum, Surfaces, and Films, 2007. 25(3): p. 543-550.**
53. **R.A. Guyer,*Rolling bearings handbook and troubleshooting guide*. 1996, New York: CRC Press - Pages 4-5.**
54. **E. Broitman, N. Hellgren, Z. Czigany, R. Twesten, J. Luning, I. Petrov, L. Hulttman, and B.C. Holloway. Journal of Vacuum Science and Technology A, 2003. 21: p. 851-859.**
55. **S.J. Bull and E.G. Berasetegui. Tribology International, 2006. 39(2): p. 99-114.**